RESEARCH PAPER

Prediction of the viscosity of water confined in carbon nanotubes

Hongwu Zhang · Hongfei Ye · Yonggang Zheng · Zhongqiang Zhang

Abstract In this paper, the viscosity of water confined in single-walled carbon nanotubes (SWCNTs) with the diameter ranging from 8 to 54 Å is evaluated, which is crucial for the research on the nanoflow but difficult to be obtained. An "Eyring-MD" (molecular dynamics) method combining the Eyring theory of viscosity with the MD simulations is proposed to tackle the particular problems. For the critical energy which is a parameter in the "Eyring-MD" method, the numerical experiment is adopted to explore its dependence on the temperature and the potential energy. To demonstrate the feasibility of the proposed method, the viscosity of water at high pressure is computed and the results are in reasonable agreement with the experimental results. The computational results indicate that the viscosity of water inside SWCNTs increases non-linearly with enlarging diameter of SWCNTs, which can reflect the size effect on the transports capability of the SWCNTs. The trend of the viscosity is well explained by the variation of the hydrogen bond of the water inside SWCNTs. A fitting equation of the viscosity of the confined water is given, which should be significant for recognizing and studying the transport behavior of fluid through the nanochannels.

Keywords Viscosity · Carbon nanotube · Confined water · Eyring theory · Molecular dynamics

H. Zhang (✉) · H. Ye · Y. Zheng · Z. Zhang
State Key Laboratory of Structural Analysis for Industrial Equipment, Department of Engineering Mechanics, Faculty of Vehicle Engineering and Mechanics, Dalian University of Technology, Dalian 116023, China
e-mail: zhanghw@dlut.edu.cn

1 Introduction

The water flow in single-walled carbon nanotubes (SWCNTs) has attracted considerable attention in recent years due to its wide potential applications (Alberto 2006; Chen et al. 2008; Holt 2008; Hummer et al. 2001; Li et al. 2010; Liu et al. 2005; Majumder et al. 2005; Thomas and McGaughey 2008), such as nanofluidic channel and drug delivery (Bianco et al. 2005; Kalra et al. 2003; Zhu et al. 2004). Previous studies have revealed that the flow rate of water transport through the SWCNTs is 3 to 5 orders of magnitude higher than the rate predicted by the classical continuum theory (Holt et al. 2006; Joseph and Aluru 2008; Majumder et al. 2005; Thomas and McGaughey 2008). These results suggest that the nanoscale surface and the geometrical confinement could cause a dramatic change in the dynamic behavior of fluid. Hence, it is crucial to investigate the unique property of the fluid in nanoconfinement.

The viscosity is an important transport property in classical continuum theory. It varies with the temperature and the pressure and can be measured by the experimental method (David 2003–2004; Hallett 1963; Wonham 1967). Furthermore, some theoretical methods and empirical formulas have also been proposed to estimate the fluid viscosity (Poling et al. 2001). Eyring et al. (Eyring 1936; Kincaid et al. 1941; Powell et al. 1941) presented the Eyring theory of viscosity which has been extensively investigated and developed to examine the temperature and pressure dependences of the viscosity (Bosse and Bart 2005; Horne et al. 1965; Lee et al. 1999; Lei et al. 1997). By using the equilibrium MD simulations, the viscosity can also be calculated by the stress-correlation function (Alfè and Gillan 1998; Balasubramanian et al. 1996; Bertolini and Tani 1995; Guo and Zhang 2001) and the

Stokes–Einstein relation (Alfè and Gillan 1998; Sun et al. 2007; Thomas and McGaughey 2008). However, these two existed methods have their intrinsic limitations and difficulties (Bertolini and Tani 1995; Powell et al. 1941; Thomas and McGaughey 2008). Besides the temperature and the pressure dependences, the viscosity is also a scale-dependent property which has been reported by a few works (Chen et al. 2008; Han et al. 2008; Liu et al. 2005; Thomas and McGaughey 2008). Nevertheless, in most previous studies on the nanoflow through the continuum theory, the viscosity of the confined water is always substituted by the viscosity of the bulk water to predict the mass flow rate (Holt et al. 2006; Joseph and Aluru 2008). The magnitude of the flow rate obtained by these calculations may be acceptable but their trends with the characteristic size of the nanochannel should be reevaluated. Thomas and McGaughey (2008) calculated the viscosity of water confined in SWCNTs with diameter ranging from 16.6 to 49.9 Å by the Stokes–Einstein relation, but in the small-diameter SWCNTs it cannot be computed due to the limitation of the relation. It is indicated that the calculation of the fluid viscosity in small nanoconfinement is an important but still unsolved problem. However, through the experiment and the theoretical formula, it is difficult to obtain the viscosity of the confined fluid due to the extremely small scale and the unpredictable state variables. As for the two MD methods, their applicability is still questionable for this special case (Thomas and McGaughey 2008; Mallamace et al. 2010). Hence, it is necessary to develop an accurate and efficient computational method for computing the viscosity of fluid at nanoscale.

In this paper, to calculate the viscosity of water inside SWCNTs, a semi-empirical formula of fluid viscosity referred to as "Eyring-MD" method is proposed on the basis of the Eyring theory and the MD simulations. The numerical experiment of the bulk water is adopted to explore the property of the undetermined critical energy. To examine the feasibility of the present method, the viscosity of the bulk water at high pressures is computed. By using this method, we predict the viscosity of water confined in SWCNTs with diameter ranging from 8 to 54 Å at 298 K, which is hardly obtained by the experimental and the existed computational methods. According to the computational results, a fitting equation which quantitatively describes the relationship between the confined viscosity and the diameter of the SWCNTs is presented, which is instructive for the further research on the nanoflow. The calculations in this paper demonstrate the correctness and the efficiency of the proposed method. Moreover, it should be emphasized that the "Eyring-MD" method can be applied to calculate the viscosity of the other fluids.

2 The "Eyring-MD" method

Eyring and his coworkers presented an explanation of the transport mechanism in the fluid based on the theory of absolute reaction rates, in which the relationship between the viscosity and the temperature is described by (Eyring 1936; Kincaid et al. 1941)

$$\eta = \frac{Nh}{V} \exp\left(\frac{E_a}{RT}\right) \tag{1}$$

where η is the shear viscosity of the fluid, N is Avogadro's number, h is Planck constant, V is molar volume, R is the gas constant and T is temperature. E_a is the activation energy, which is a potential occasionally acquired by an individual molecule to overcome the potential barrier and squeeze past its neighbors into the next equilibrium position (Powell et al. 1941). It is difficult to be directly obtained through the experimental and the computational methods. Generally, the activation energy is related to the heat of vaporization which has been extensively studied (Kincaid et al. 1941). It can also be expressed as a function of the state variables and undetermined coefficients in some empirical formulas (Bosse and Bart 2005; Lee et al. 1999; Lei et al. 1997). Moreover, in physical chemistry, the nudged elastic band method based on the transition state theory is commonly utilized to calculate the activation energy (Henkelman and Jónsson 2000). With use of this method, the viscosity of the bulk water calculated by Eq. 1 has an obvious deviation from the result calculated by the Stokes–Einstein relation. This may be because that the physical meaning of the activation energy in the transition state theory is different from that in the Eyring theory. Tolman (1920) proposed an explanation of the activation energy from the viewpoint of the statistical mechanics. For all the molecules in the system, only a portion of them are in the activated state, and the activation energy E_a equals to the difference between the average energy of the activated molecules ($\bar{E}_{act}$) and the average energy of all the molecules ($\bar{E}$), i.e.,

$$E_a = \bar{E}_{act} - \bar{E} \tag{2}$$

The activated molecules are the portion whose potential energies larger than a critical value E_c, as shown in Fig. 1. This critical value E_c represents the potential energy's lower limit of the activated molecules and thereby is called the critical energy.

In MD simulations, the molecular potential energy is stable and can be easily calculated. Moreover, the Eyring theory is a computational model based on the molecular motion and can be developed to calculate the viscosity of the unimolecular films (Kauzmann and Eyring 1940; Walter et al. 1938), which implies that it is still an available tool on the molecular level. Thus, it is expected that the

Eyring theory may also be developed in combination with the MD simulations, which should be effective for the calculations of the viscosity of nanofluid. Figure 1 shows the probability distributions of the potential energies of water molecules at 250, 298, 350, and 400 K (symbol) calculated by the MD simulations in the micro-canonical ensemble (NVE). Some representative simulations are also performed in the canonical ensemble (NVT), in which the probability distributions of the potential energies exhibit similar profiles. From Fig. 1, it is found that the probability distributions of the molecular potential energies can be well fitted by the Gaussian distribution function (line) which may not reflect the real physical fundament but is accurate and simple to be computed. The error of the fittings decreases with increasing temperature, and the largest error is about 1.5% occurs at 250 K and the average error for all the calculations is about 0.9%. Hence, we assumed that the Gaussian distribution can describe the probability density of the water potential energy, i.e.,

$$f(E) = \frac{1}{\sqrt{2\pi}\sigma} \exp\left[-\frac{(E - \bar{E})^2}{2\sigma^2}\right] \quad -\infty < u < \infty \quad (3)$$

where E is the potential energy occupied by a water molecule, and σ is the standard deviation of the potential energies. Then, with use of Eqs. 2 and 3, we can obtain

$$E_a = \int_{E_c - \bar{E}}^{\infty} E \exp\left(-\frac{E^2}{2\sigma^2}\right) dE \bigg/ \int_{E_c - \bar{E}}^{\infty} \exp\left(-\frac{E^2}{2}\right) dE \quad (4)$$

For Eq. 4, the analytical expression of E_a can not be obtained due to the Gaussian integral with a finite lower bound, i.e., $\Phi(x) = \int_{E}^{\infty} \exp(-x^2/2) dx$. Here, this integral is calculated by an approximate formula as follows (Bryc 2002)

$$\Phi(E) \approx \begin{cases} \sqrt{2\pi} \exp\left(-\frac{E^2}{2}\right) \frac{E + g_1}{\sqrt{2\pi E^2 + g_2 E + 2g_1}}, & E > 0 \\ \sqrt{2\pi}\left[1 - \exp\left(-\frac{E^2}{2}\right) \frac{g_1 - E}{\sqrt{2\pi E^2 - g_2 E + 2g_1}}\right], & E \leq 0 \end{cases} \quad (5)$$

where $g_1 = 3.333$ and $g_2 = 7.32$. The largest relative error of Eq. 5 is 2.3% and occurs in the range of $4.8 \leq E \leq 7.8$. Then, the activation energy E_a can be expressed as follows
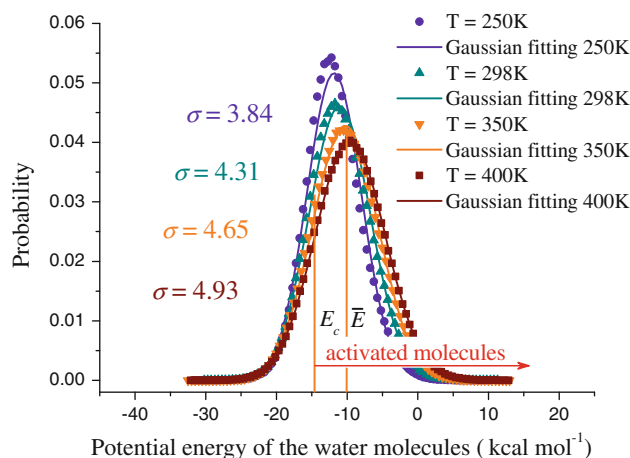

Fig. 1 The probability distributions of potential energies occupied by the water molecules and the Gaussian distribution fittings

$$E_a = \begin{cases} \dfrac{\sigma\left[\sqrt{2\pi}(E_c - \bar{E})^2/\sigma^2 + g_2(E_c - \bar{E})/\sigma + 2g_1\right]}{\sqrt{2\pi}(E_c/\sigma - \bar{E}/\sigma + g_1)}, & E_c > \bar{E} \\ \sigma \bigg/ \left[\sqrt{2\pi}\exp\left(\dfrac{(E_c - \bar{E})^2}{2\sigma^2}\right) - \dfrac{\sqrt{2\pi}(\bar{E}/\sigma - E_c/\sigma + g_1)}{\sqrt{2\pi}(E_c - \bar{E})^2/\sigma^2 - g_2(E_c - \bar{E})/\sigma + 2g_1}\right], & E_c \leq \bar{E} \end{cases} \quad (6)$$

Hence, two expressions of the activation energy E_a are obtained based on the potential energy, the distribution and the undetermined critical energy E_c. According to Eq. 1, the water viscosity can be expressed as

$$\eta = \begin{cases} \dfrac{Nh}{V} \exp\left\{\dfrac{\sigma\left[\sqrt{2\pi}(E_c - \bar{E})^2/\sigma^2 + g_2(E_c - \bar{E})/\sigma + 2g_1\right]}{RT\sqrt{2\pi}(E_c/\sigma - \bar{E}/\sigma + g_1)}\right\}, & E_c > \bar{E} \\ \dfrac{Nh}{V} \exp\left\{\sigma \bigg/ RT\left[\sqrt{2\pi}\exp\left(\dfrac{(E_c - \bar{E})^2}{2\sigma^2}\right) - \dfrac{\sqrt{2\pi}(\bar{E}/\sigma - E_c/\sigma + g_1)}{\sqrt{2\pi}(E_c - \bar{E})^2/\sigma^2 - g_2(E_c - \bar{E})/\sigma + 2g_1}\right]\right\}, & E_c \leq \bar{E} \end{cases} \quad (7)$$

Thus, a formula on the basis of the Eyring theory and some quantities associated with the potential energy in MD simulations is proposed and therefore is referred to as "Eyring-MD" method. It should be noted that the activation energy calculated by the first formula in Eq. 6 $(E_c > \bar{E})$ has a lower limit of $\sqrt{2\pi}\sigma/\pi$ that is larger than most activation energies of water in gaseous, liquid and even solid state computed in this paper. Therefore, the second equations in Eqs. 6 and 7 are valid in most cases. Furthermore, it can be found that an undetermined value E_c still exists in Eq. 7. In this paper, the numerical experiment is adopted to explore the property of the critical energy E_c, where E_c is calculated by Eq. 7 and the MD simulations of

bulk water. The viscosity of bulk water is obtained from the Stokes–Einstein relation. We adopt a modification that the radius of the first peak in the radial distribution function (RDF) is chosen to be the diameter of water molecule, which can greatly improve the computational accuracy of the viscosity (Alfè and Gillan 1998). Through the numerical experiments, we respectively examine the dependence of the critical energy on the temperature, the van der Waals energy and the coulomb energy. It is expected that the critical energy E_c can be expressed as a function of the known values and a semi-empirical formula can be proposed to compute the viscosity of water confined in SWCNTs.

3 The research on the critical energy E_c

3.1 The numerical experiment

The simulations are performed by an open-source MD code LAMMPS (Steve 1995). The computational model includes 906 water molecules in a simulation box with an initial density of 1.0 g/cm^3, as shown in Fig. 2. The periodic boundary condition is applied to all the three directions and
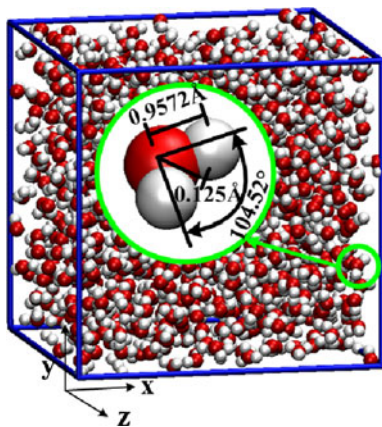

Fig. 2 The computational model of the numerical experiment

the particle–particle particle–mesh (pppm) algorithm is adopted to handle the long-range coulomb interactions. The time step is 1 fs. The TIP4P-EW water model (Fig. 2) is employed to compute the potential energy with the main parameters $\sigma_{OO} = 3.16435$ Å, $\varepsilon_{OO} = 0.16275$ kcal mol^{-1}, $q_O = -1.04844e$, and $q_H = 0.52222e$, where e is the elementary charge (Hans et al. 2004). The SHAKE algorithm is used to constrain the bond and the angle of the water to the specified values. In this paper, we refer to the Lennard-Jones (LJ) potential including the van der Waals interaction and a nuclear repulsion as the van der Waals energy. The cutoff distance for the LJ interactions and the electronic interactions are 10 and 12 Å, respectively. The simulation process can be divided into three steps. Firstly, it is conducted in the isothermal–isobaric ensemble (NPT) for 80 ps at 1 atm to obtain the average density of the water. Then, the system is equilibrated for 40 ps in the NVT, in which the volume of the simulation box is reset according to the average density in step 1. Finally, the data is collected in the NVE within 320 ps. The constant temperature and the constant pressure are controlled by the Nose/Hoover temperature thermostat and pressure barostat, respectively. The results in this work are averaged by three repeat runs for each case to eliminate the influence of the initial velocity and configuration.

The parameters for the three numerical experiments are displayed in Table 1. Through the numerical experiment of the temperature dependence, we explore the property of the critical energy of the bulk water. Furthermore, for the water confined in SWCNTs, due to the change in the microstructure of the water close to the tube wall and the presence of the interactions between the carbon atoms and the water molecules, the van der Waals energy and the coulomb energy are different from those of the bulk water. Hence, the influences of these energies on the critical energy need to be considered and investigated. These two numerical experiments are conducted by using another four depths of potential well $\varepsilon = 0.75\varepsilon_{OO}$, $1.25\varepsilon_{OO}$, $1.5\varepsilon_{OO}$, $1.75\varepsilon_{OO}$ and two atom charges $q = 0.967q_0$, $1.033q_0$ (at 250, 298, and 350 K), where ε_{OO} is the initial depth of

Table 1 The numerical experiments for the critical energy E_c

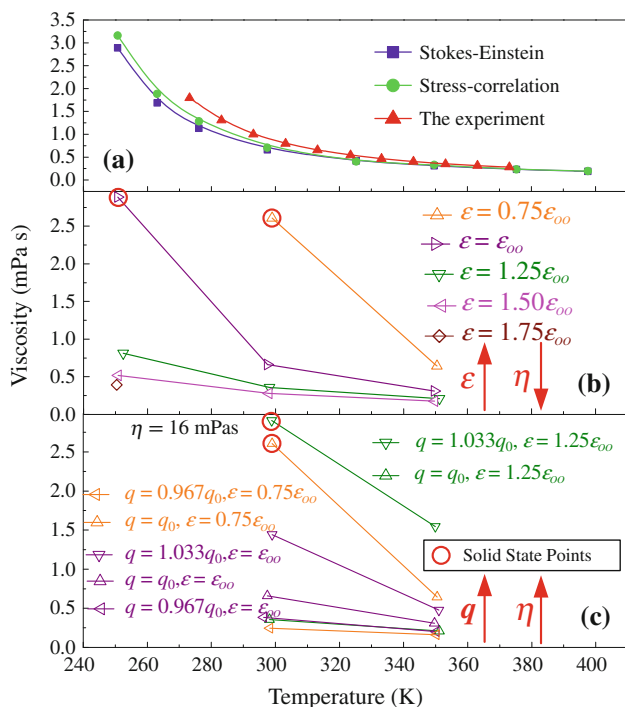| Numerical experiment	Temperature (K)	The depth ε (ε_{OO})	The charge q (q_0)
Temperature dependence	250.0, 262.5, 275.0, 298.0, 325.0, 350.0, 375.0, 400.0	1.00	1.00
Van der Waals energy dependence	250.0	1.00, 1.25, 1.5, 1.75	1.00
	298.0	0.75, 1.00, 1.25, 1.5	1.00
	350.0	0.75, 1.00, 1.25, 1.5	1.00
Coulomb energy dependence	298.0, 350.0	0.75	0.967
	298.0, 350.0	1.00	0.967, 1.033
	298.0, 350.0	1.25	1.033

Fig. 3 **a** The viscosity of water with the initial parameters ε_{OO} and q_0 against the temperature. **b** The viscosity of water with the different depths of potential well ε and initial atom charge q_0 against the temperature. **c** The viscosity of water with the different atom charges q against the temperature

potential well in LJ interaction and q_0 is the initial charge of oxygen and hydrogen atoms in coulomb interaction.

Figure 3a shows the viscosity of the bulk water with the initial parameters ε_{OO} and q_0 calculated by the methods from the Stokes–Einstein relation and the stress-correlation function. The difference between them decreases with increasing temperature and is about 6% on average. The experimental results (David 2003–2004) are also given in Fig. 3a, which are consistent with the present simulation results. The viscosities of 2.89 mPa s at 250.7 K and 0.66 mPa s at 297.5 K are comparable with those of 2.14 ± 0.2 mPa s at 245 K, 0.47 ± 0.07 mPa s at 298 K (Bertolini and Tani 1995) and 0.66 ± 0.08 mPa s at 303.15 K (Balasubramanian et al. 1996) calculated by the stress-correlation function through the MD simulations. Meanwhile, the viscosity of water with the different depths of potential well ε and atom charges q is also displayed in Fig. 3b and c, respectively. For a given temperature, the viscosity of water with the same charge decreases with increasing depth of potential well ε, whereas the viscosity of water with the same depth of potential well increases with increasing atom charge q. These variations of the viscosity can be well explained by the different contributions of the van der Waals energy and the coulomb energy in the viscous flow of water. For two neighboring water

molecules, the van der Waals energy (LJ interaction) mainly plays repulsive roles because the average distance between the water molecules is shorter than the LJ parameter σ_{OO}, whereas the coulomb energy mainly plays attractive roles due to the self-assemble ability of polar water molecules. As the depth of potential well ε increases, the contribution of the van der Waals energy is more significant and the interactions between two neighboring water molecules are weakened, which can result in a decrease in the water viscosity. Similarly, as the atom charge q increases, the increasing coulomb energy enhances the interactions, which can result in an increase in the water viscosity. Furthermore, it can be observed that there are three viscosities remarkably higher than the other values, as denoted as "Solid State Points" in Fig. 3. From their extremely large viscosities, it can draw that the water in these three points are in solid state. They can be seen as fragile liquid (Angell 1993; Velikov et al. 2001) in which the exponential relationship between the viscosity and the reciprocal of temperature is no longer valid. This point can also be demonstrated in the following calculation. The large viscosity of 16 mPa s as labeled in Fig. 3c is the only case whose activation energy higher than the lower limit $\sqrt{2\pi}\sigma/\pi$ of the first equation in Eq. 6.

3.2 The critical energy E_c

As can be seen from Eq. 7, the viscosity depends on the ratio of the critical energy E_c to the standard deviation σ. So it is supposed that the critical energy may be related to the standard deviation. Figure 4 plots the critical energy E_c as a function of the standard deviation σ. For the numerical experiments with use of the initial parameters ε_{OO} and q_0 (temperature dependence), it is observed that the critical energy decreases nonlinearly from −12.9 to −13.8 kcal mol^{-1} as the temperature increases, and only a slight change can be detected when the temperature is larger than 298 K, as shown in Fig. 4a. Hence, the critical energy can be seen as a constant approximately in the calculation of the viscosity of liquid or gaseous water. As the temperature decreases from 298 to 250 K, the water is in the transition from the liquid state to the solid state and the water molecules gradually exhibit an ordered configuration which is similar to the arrangement of the water layers near the wall of SWCNTs (Joseph and Aluru 2008; Mashl et al. 2003; Walther et al. 2001). In addition, compared with the potential energy of the bulk water, the potential energy of the water in the above boundary layers is also changed. Hence, to calculate the viscosity of water inside SWCNTs, the property of the critical energy at low temperature and its variation with the potential energy still require further research.
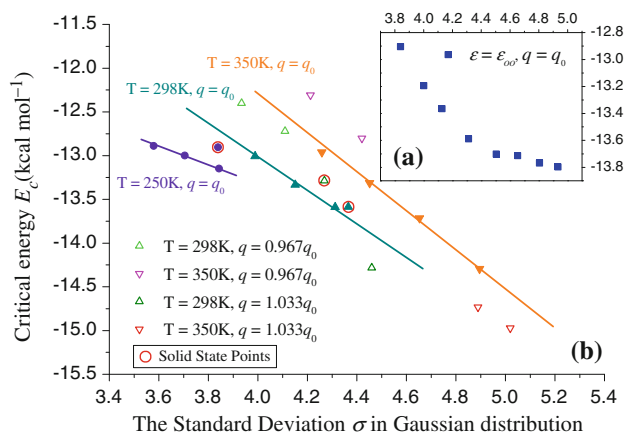
Fig. 4 **a** The critical energy of water with the initial parameters ε_{OO} and q_0 versus the standard deviation σ in Gaussian distribution. **b** The relationship between the critical energy of water with the different parameters and the standard deviation σ in Gaussian distribution

Fig. 5 The relationships between the coulomb energy and the van der Waals energy

Figure 4b presents the critical energy of water with the different depths of potential well ε and atom charges q at 250, 298, and 350 K. For the water with the initial charge q_0 and the different depths ε, the critical energy is almost linearly dependant on the standard deviation σ at the same temperature. When the atom charge is changed by ± 0.033 q_0, the critical energies deviate from the above linear relations with approximately the same distances. Take the samples at 350 K as an example (downward triangle), when the atom charge is changed from q_0 (symbols on the line) to 0.967 q_0 (symbols above the line), the critical energy has an increment relative to the line. The reason of the discrepancies is that the critical energy which is used to calculate the water viscosity relies on the cooperative effect of the van der Waals energy and the coulomb energy. For the water in which only the depth of potential well is changed, the ratio of the two energies is dramatically different from that for the water in which only the atom charge is changed. Such difference between the ratios will result in a discrepancy of the critical energy considering the influence of the coulomb energy from the line representing the influence of the van der Waals energy.

To correct the discrepancies of the critical energy from the lines, the relationships between the van der Waals energy and the coulomb energy at 298 and 350 K are investigated, as shown in Fig. 5. For the different depths of potential well ε and the initial atom charge q_0, the coulomb energy is as an approximately linear function of the van der Waals energy as follows

$$U_{\mathrm{coul}} = p_1 U_{\mathrm{van}} + p_2 \qquad (8)$$

where U_{coul} and U_{van} is the coulomb energy and the van der Waals energy which follow the linear relations, $p_1 = -2.062576$ and $p_2 = -8.984223$ kcal mol^{-1} at 298 K, $p_1 = -2.065280$ and $p_2 = -8.502127$ kcal mol^{-1} at 350 K.
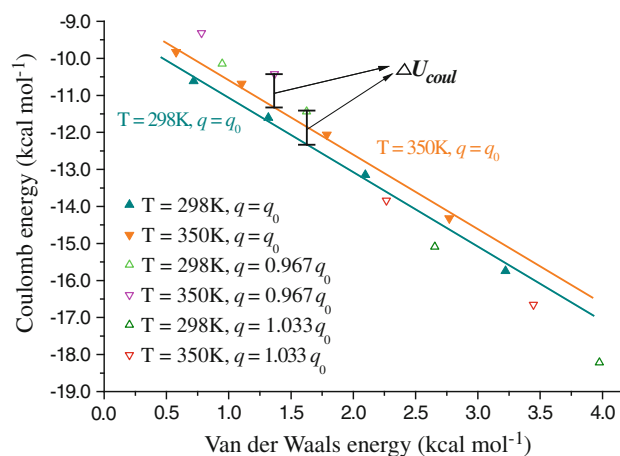
From Fig. 5, it can be seen that when the atom charge q is changed, some discrepancies from the straight lines (Eq. 8) can be observed, which are similar to the variations in Fig. 4b. Therefore, along with the description mentioned above, it is considered that the anomalous variations of the critical energy induced by the changed atom charges q in Fig. 4b can be corrected by the difference ΔU_{coul} between the coulomb energy from the MD simulations and that from Eq. 8. This correction of the critical energy reflects the influence arises when the variation of the coulomb energy dominates over the variation of the van der Waals energy (deviate from the lines). Actually, such correction is a resistance to the variation of the viscosity. Take $T = 350$ K and $q = 0.967q_0$ as an example, for a given depth of potential well ε, the critical energy without the correction is lower than that has been corrected, as shown in Fig. 4b. For the same standard deviation, the lower critical energy implies the smaller water viscosity because the average potential energy of the activated molecules is closer to that of all the molecules. Thus, the above correction term which enhances the critical energy will resist the decrease in the water viscosity.

Furthermore, it can be seen that the critical energies denoted as "Solid State Points" in Fig. 4b deviate from the predictions. It implies the breakdown of the exponential relationship which is consistent with the description of the fragile fluid. Hence, the "Eyring-MD" method will underestimate the viscosity of the icy and the glassy water and is applicable for the gaseous and liquid water.

According to the simulation results mentioned above, four assumptions about the critical energy can be proposed as follows: (1) The critical energy E_c is as a function of the temperature T and the standard deviation σ in the Gaussian distribution. (2) The critical energy E_c is linearly dependant on the standard deviation σ at the same temperature. (3) The slope and the intercept of the E_c–σ lines (assumption

(2)) are as a linear function of the temperature. (4) The increment or decrement in the critical energy arises when the variation of the coulomb energy dominates over the variation of the van der Waals energy is in proportion to the discrepancy ΔU_{coul}. Thus, the critical energy can be given by

$$E_c = (aT + b)\sigma + (cT + d) + e\Delta U_{\text{coul}} \qquad (9)$$

where a, b, c, d, and e are the fitting coefficients and $a = -0.002171\ \text{K}^{-1}$, $b = -1.114322$, $c = 0.018546\ \text{kcal mol}^{-1}\ \text{K}^{-1}$, $d = -11.486829\ \text{kcal mol}^{-1}$ and $e = 0.63$ from our calculations. The last term in Eq. 9 is the correction of the critical energy which can be almost ignored for a specified matter in the general case. But for the viscosity of water confined in SWCNTs, the effect of this correction term should be considered. By using Eqs. 7 and 9, the viscosity of water can be expressed as a function of the temperature and some statistical quantities from the MD simulations including the potential energy and its distribution. It is referred to as "Eyring-MD" method and can be seen as a semi-empirical formula. This method can be utilized to calculate the viscosity of water confined in SWCNTs because the potential energy is a stable quantity in the MD simulations. The proposed method may be also applicable for the other fluid through carrying out similar preparative works as above. Three advantages of the "Eyring-MD" method are summarized as follows: Firstly, if the undetermined coefficients are obtained, the cost of the calculation of viscosity will be very low. Secondly, compared with the empirical formulas, the present method still needs few calculations to obtain the potential energy, but it can obtain more accurate results. Finally, the proposed method could be used to calculate the viscosity of fluid in some special case, for instance, the water confined in SWCNTs.

4 Results

4.1 Bulk water at high pressure

To demonstrate the validity of the "Eyring-MD" method, the variations of the relative viscosity of water with the pressure at 298 and 350 K are examined. The relative viscosity is the ratio of the water viscosity at a specified pressure to that at 1 atm, i.e., $\eta_r = \eta_P/\eta_1$. Here, $\eta_1 = 0.676$ mPa s at 298 K and $\eta_1 = 0.309$ mPa s at 350 K. Figure 6 shows the relative viscosity calculated by the "Eyring-MD" method (solid symbol) and the Stokes–Einstein relation (open symbol). The experimental results (solid line) and their extrapolations (dashed line) are also displayed in the figure (Wonham 1967). It is found that the variations of the water viscosity with the pressure are not obvious due to the incompressibility of water. From the
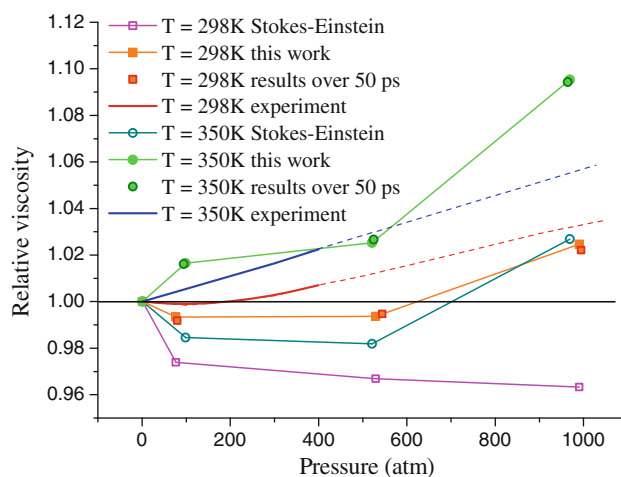

Fig. 6 The relative viscosity of water at high pressure obtained by the "Eyring-MD" method, the Stokes–Einstein relation and the experiment

experimental results, it can be seen that the relative viscosity slightly decreases initially and then increases with increasing pressure at 298 K, while the relative viscosity is almost in proportional to the pressure at 350 K. The differences between the experimental results and the computational results from the "Eyring-MD" method and the Stokes–Einstein relation are about 1.4 and 3.8%, respectively. While the results from the "Eyring-MD" method can better describe the trend than the results from the Stokes–Einstein method. Though the coefficients in this semi-empirical method are obtained through the viscosity calculated by the Stokes–Einstein relation, the present method can compute the trend more accurately because its required quantities (potential energy and standard deviation) are more stable in the MD simulations. In Fig. 6, the viscosity calculated over a short time period of 50 ps is also presented. The differences between the results from the long time simulations and those from the short time simulations are about 0.1% on average. Thus, the run time of 50 ps is adequate for the calculation of viscosity by using the "Eyring-MD" method, which is much shorter than the typical sampling time of the stress-correlation function and the Stokes–Einstein relation.

4.2 Confined water

In this section, the viscosity of water confined in SWCNTs at 298 K is calculated. The parameters for the LJ interaction between the carbon and the oxygen atoms are $\sigma_{\text{CO}} = 3.28218\ \text{Å}$ and $\varepsilon_{\text{CO}} = 0.11831\ \text{kcal mol}^{-1}$. The carbon atoms of SWCNTs are fixed in the simulations to save the computational cost. We adopt the periodic boundary in all the directions. The illustrations of the three computational models are shown in Figs. 7 and 8 and their detailed sizes are
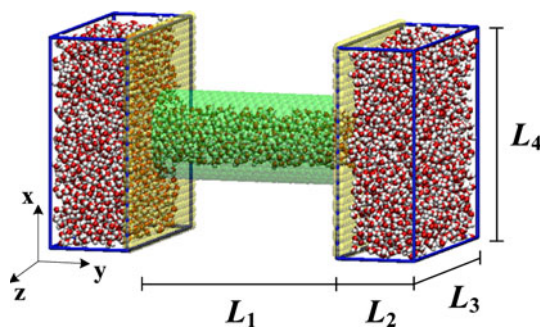
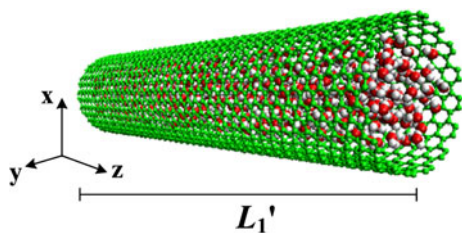**Fig. 7** The schematic illustration of the computational model in step 1

Fig. 8 The schematic illustration of the computational model in steps 2 and 3

Table 2 The sizes of the computational models in steps 1, 2, and 3

Chirality	Radius (Å)	Step 1				Steps 2 and 3
		L_1 (Å)	L_2 (Å)	L_3 (Å)	L_4 (Å)	L_1' (Å)
(6, 6)	4.07	60.26	20.00	29.82	29.51	2361.13
(7, 7)	4.75	60.26	20.00	29.82	29.51	1234.06
(8, 8)	5.42	60.26	20.00	29.82	29.51	683.74
(9, 9)	6.10	60.26	20.00	29.82	29.51	506.66
(10, 10)	6.78	60.26	20.00	34.08	36.89	371.39
(11, 11)	7.46	60.26	20.00	34.08	36.89	292.68
(12, 12)	8.14	60.26	20.00	42.60	41.81	226.28
(16, 16)	10.85	60.26	20.00	59.03	59.66	110.68
(20, 20)	13.56	60.26	20.00	76.68	76.25	103.3
(24, 24)	16.27	60.26	20.00	85.72	83.62	98.38
(30, 30)	20.34	60.26	20.00	98.38	97.98	88.54
(40, 40)	27.12	60.26	20.00	123.54	125.44	78.70

listed in Table 2. The MD simulation is conducted in the NVT ensemble and can be divided into three steps. Firstly, a computational model including a SWCNT and two water reservoirs is equilibrated for 80 ps (Fig. 7), and the water density in the reservoirs away from the tube is maintained 0.99 g/cm^3 (density of the bulk water at 298 K). The objective of the present step is to calculate the amounts of the water molecules in the various SWCNTs (Table 3). Secondly, the two water reservoirs are removed, and a SWCNT are adopted as the second model to equilibrate for 100 ps (Fig. 8). The amounts of the water molecules in SWCNTs

are determined from the results of step 1. Finally, based on the second model, the data is collected within 500 ps. The other settings for the present MD simulations are same to those for the numerical experiments.

Figure 9 shows the relative viscosity of water (solid circle) inside SWCNTs at 298 K calculated by the "Eyring-MD" method versus the diameter. Here, the relative viscosity is the ratio of the viscosity of water confined in SWCNTs to the viscosity of the bulk water, i.e., $\eta_r = \eta_{cnt}/\eta_{bulk}$, where $\eta_{bulk} = 0.676$ mPa s. The relative viscosity depicts the variation of the viscosity of the confined water relative to the viscosity of the bulk water. Meanwhile, it makes the comparison between the present computational results and the other results more clear. It can be seen that the relative viscosity of water inside SWCNTs increases nonlinearly with enlarging diameter. Three different regions can be clearly distinguished according to the trend of the water viscosity. The first region is the molecule-governed region ($d < 10.5$ Å), in which the water viscosity increases dramatically with an increase in the diameter of SWCNTs. In this region, the flow is controlled by the individual motions of the water molecules and the continuum theory may be invalid for calculating the flow rate. But the viscosity presented in Fig. 9 still reflects the transport capacity of the SWCNTs with the extremely small diameter, i.e., the high-speed conduction which has been widely reported. The second region is the transition region ($d = 10.5–14.5$ Å), in which the variation of water viscosity with the diameter becomes slow while the water molecules undergo a transition from the individual behaviors to the collective motions. The last region is the continuum region ($d > 14.5$ Å), in which the curve gradually flattens and the viscosity of the confined water approaches that of the bulk water. Here, the water can be seen as a continuum approximately and some modified microflow theories may be valid. According to the simulation results, the relative viscosity of water confined in SWCNTs is fitted as follows

$$\eta = \eta_{bulk} \left[1 - \left(\frac{5.14}{d} \right)^{0.7} + \left(\frac{10.02}{d} \right)^{2.9} - \left(\frac{9.65}{d} \right)^{3.9} \right]$$

(10)

where d is the diameter of the SWCNTs. The relative viscosity calculated by Eq. 10 is also depicted in Fig. 9. The proposed formula should be significant for the researches on the water transport through the SWCNTs and the design of nanofluidic channels. At the same time, the results over 50 ps (small solid circle) are also shown in Fig. 9, and the average difference between the long time and the short time simulations is about 0.4%.

The hydrogen bond of the water inside SWCNTs is also studied to further understand the variation of the water

Table 3 The amounts of the water molecules inside SWCNTs

Chirality	Step 1 (L_1)				Steps 2 and 3 (L_1')
	Amount[a]	Amount[b]	Initial amount	Amount in equilibrium	Amount for steps 2 and 3
(6, 6)	22	23	22	22	862
(7, 7)	–	48	48	44	901
(8, 8)	75	74	75	80	908
(9, 9)	–	106	106	108	908
(10, 10)	141	146	143	146	900
(11, 11)	–	186	185	188	913
(12, 12)	242	239	241	240	901
(16, 16)	475	492	483	496	911
(20, 20)	748	838	790	840	1440
(24, 24)	–	1257	1200	1293	2111
(30, 30)	–	2043	1950	2120	3115
(40, 40)	–	3935	3850	3998	5221

[a] Hanasaki and Nakatani (2006)
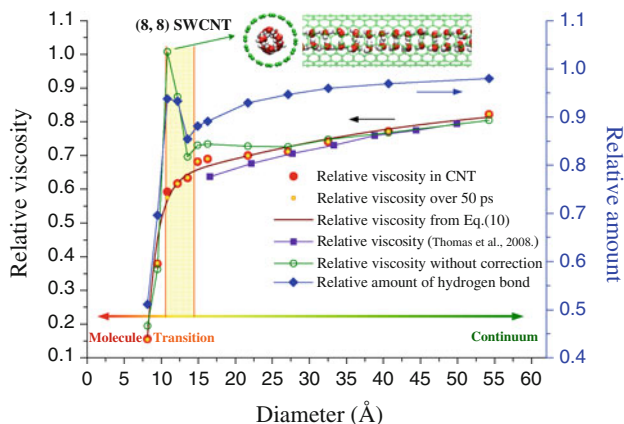
[b] Alexiadis and Kassinos (2008)

Fig. 9 The relative viscosity of water, the previous results, the uncorrected results, the relative amount of the hydrogen bonds against the tube diameter

viscosity with the diameter. It is well known that the hydrogen bond is an important intermolecular bond in water (Alenka and David 1996). The computational results of the relative amounts of the hydrogen bonds (solid diamond) are shown in Fig. 9. The relative amount is defined as the ratio of the amount of the hydrogen bonds of the confined water to that of the bulk water, i.e., $N_r = N_{cnt}/N_{bulk}$, where $N_{bulk} = 3.494$. The geometrical criterion (Martí 1999) is adopted to calculate the hydrogen bond and the results are in good agreement with those calculated by Hanasaki and Nakatani (2006) and Martí (1999). From Fig. 9, it can be seen that all the relative amounts are lower than 1, which means that the amount of the hydrogen bonds of the confined water is lower than that of the bulk water. Some previous works have pointed out that, compared with the bulk water, the water confined in SWCNTs have energy loss owing to the breakings of the hydrogen bonds, and only a portion of them can be recovered through the van

der Waals interactions between the water molecules and the carbon atoms of SWCNTs (Hummer et al. 2001; Wang et al. 2008). It is suggested that the combinations among the water molecules especially for those close to the tube wall are weakened, which could result in a relatively low viscosity. This is consistent with the present results of the viscosity of the confined water. A similar presentation is also given by Han et al. (2008) to explain the decrease in the effective viscosity of the glycerin inside nanopores. From Fig. 9, it can be observed that the trend of the relative amount of the hydrogen bonds is almost similar to the trend of the relative viscosity except in the (8, 8) and the (9, 9) SWCNTs whose magnitude are higher than their adjacent results. The discontinuity in the relative amount of the hydrogen bonds is because that the water molecules exhibit a close, ordered and hollow arrangement in the (8, 8) and the (9, 9) SWCNTs at 298 K. The front and the side views of the water molecules in the (8, 8) SWCNT are shown in Fig. 9. Corresponding to the abnormal increment in the curve of the hydrogen bond, the smoothness of the viscosity can be explained by the effect of the correction term of the critical energy. Without utilizing the correction term, the relative viscosity of the water inside SWCNTs (open circle) has a remarkable increment in the transition region, which is similar to the curve of the relative amount of the hydrogen bonds. Nevertheless, it should be noticed that the correction terms for the (8, 8) and the (9, 9) SWCNTs are quite large because there is an obvious relative variation between the van der Waals energy and the coulomb energy, which is induced by the structured configuration of the water molecules. Hence, the increase in the viscosity in the transition region is greatly resisted by the correction term and a smooth curve of the relative viscosity is obtained. The present role of the correction term can also be understood by the fact that as the distance decreases, the

van der Waals energy increases more quickly than the coulomb energy due to its stronger dependence on the distance. The increase in the van der Waals energy reduces the viscosity of the confined water. Furthermore, it should be noted that the structured configuration of the water molecules in the (8, 8) and the (9, 9) SWCNTs are similar to that in ice. However, some studies have revealed that the phase states of water in these cases at room temperature may be not yet solid (Giovambattista et al. 2009; Mashl et al. 2003) and the formation of the ice still requires lower temperature or the other conditions (Bai et al. 2006; Koga et al. 2001). Thus, the viscosity for the (8, 8) and the (9, 9) SWCNTs calculated in this work may be slightly underestimate but still acceptable.

Some previous works also reported the viscosity of water inside SWCNTs. Chen et al. (2008) and Han et al. (2008) measured the viscosity of the fluid inside the nanopores with the diameter in the range of 20–100 Å. The results reveal a decrease in the viscosity, which qualitatively validate the present results. Thomas and McGaughey (2008) computed the viscosity of water confined in SWCNTs with the diameter ranging from 16.6 to 49.9 Å using the Stokes–Einstein relation. The viscosity of the bulk water they obtained is 1.02 mPa s at 298 K, which is higher than 0.676 mPa s from our simulations. The reason is that the molecular diameter in Thomas's work is 1.7 Å, which is lower than 2.78 Å on average used in this work. (As mentioned above, we adopt the radius of the first peak in RDF as the molecular diameter (Alfè and Gillan 1998).) The relative viscosity can bypass the discrepancy of the viscosities of the bulk water which is induced by the different molecular diameters. From Fig. 9, it can be seen that the relative viscosity of water inside SWCNTs obtained in the present work (solid circle) is in good agreement with the results calculated by Thomas and McGaughey (solid square). However, the viscosity of water inside the small-diameter SWCNTs (<16.6 Å) is not given, which is due to the breakdown of the Stokes–Einstein relation in this case. Comparatively, the "Eyring-MD" method can tackle this problem because its required quantities are the potential energy and the distribution which are stable and easily obtained in the MD simulations. Chen et al. (2008) calculated the viscosity of water flow through the SWCNTs with the diameter varying from 13.5 to 81.1 Å using the shear stress and the continuum theory. The results show that when the flowing velocity is enough high, the viscosity of water inside SWCNTs will be stationary and increases with an increase in the diameter. This conclusion is also consistent with the present results. The viscosity of water confined in small SWCNTs (10.8–21.7 Å) with the specified densities was investigated by Liu et al. (2005) through the stress-correlation function. It is indicated that for the confined water with the same density, the viscosity

decreases with enlarging diameter. While for the confined water inside a given SWCNT the viscosity increases with increasing water density. These results are different from the present results. This is because that the density of the confined water in their calculation is kept as a constant for all the SWCNTs. Nevertheless, the density in the present work is determined according to the capability of the SWCNTs which is calculated by the MD simulations (step 1). In addition, when the stress-correlation function is used to calculate the viscosity of the water confined in SWCNTs, only the component of the stress tensor in the flow direction can be considered (Liu et al. 2005). It may reduce the precision of the calculation of the viscosity.

5 Conclusion

Based on the Eyring theory and the numerical experiments through the MD simulations, a semi-empirical formula referred to as "Eyring-MD" method was proposed to calculate the viscosity of water confined in SWCNTs. The numerical experiments are performed with consideration of the effects of the temperature, the van der Waals energy and the coulomb energy, respectively. The research indicates that the van der Waals energy (LJ interaction) and the coulomb energy between the two neighboring water molecules play a repulsive and an attractive role, respectively. According to the numerical experiments, we proposed an assumed expression of the critical energy E_c. The present method should be applicable for the gaseous, the liquid and perhaps some supercooled water (>262 K) but may underestimate the viscosity of the ice and the glassy water. To justify the "Eyring-MD" method, the viscosity of the bulk water at high pressure was computed. Compared with the experiment, the small difference and the similar trend validate the correctness of the proposed method. Furthermore, the efficiency can also be confirmed by a 50 ps MD simulation. Then, by using the proposed method, the viscosity of water confined in SWCNTs at 298 K was investigated and the results show that it increases nonlinearly with enlarging diameter of SWCNTs, which is in good agreement with the previous experiments and computational results. Furthermore, the amount of the hydrogen bonds of the confined water is also studied to further understand the trend of the viscosity. It is indicated that the trend of the relative amount of the hydrogen bonds is similar to that of the relative viscosity except in the transition region. The discontinuity of the relative amount is due to the structured configuration of the water molecules in the (8, 8) and the (9, 9) SWCNTs. The calculation of the viscosity demonstrates the correctness and the efficiency of the "Erying-MD" method. But it still requires more modifications and further researches to extend the

applications to the ice, the glassy water and the other fluid, such as the research on the critical energy E_c and the calculation of the activation energy E_a. The results of the viscosity and the hydrogen bond computed in this paper should be significant for recognizing the transport property of the nanofluid inside SWCNTs.

References

Alberto S (2006) The mechanism of water diffusion in narrow carbon nanotubes. Nano Lett 6(4):633–639. doi:10.1021/nl052254u

Alenka L, David C (1996) Hydrogen-bond kinetics in liquid water. Nature 379(4):55–57. doi:10.1038/379055a0

Alexiadis A, Kassinos S (2008) The density of water in carbon nanotubes. Chem Eng Sci 63:2047–2056. doi:10.1016/j.ces.2007.12.035

Alfè D, Gillan M (1998) First-principles calculation of transport coefficients. Phys Rev Lett 81(23):5161–5164. doi:10.1103/PhysRevLett.81.5161

Angell CA (1993) Water II is a strong liquid. J Phys Chem 97:6339–6341. doi:10.1021/j100126a005

Bai J, Wang J, Zeng XC (2006) Multiwalled ice helixes and ice nanotubes. Proc Natl Acad Sci 103(52):19664–19667. doi:10.1073/pnas.0608401104

Balasubramanian S, Mundy CJ, Klein ML (1996) Shear viscosity of polar fluids: molecular dynamics calculations of water. J Chem Phys 105(24):11190–11195. doi:10.1063/1.472918

Bertolini D, Tani A (1995) Stress tensor and viscosity of water: molecular dynamics and generalized hydrodynamics results. Phys Rev E 52(2):1699–1710. doi:10.1103/PhysRevE.52.1699

Bianco A, Kostarelos K, Prato M (2005) Applications of carbon nanotubes in drug delivery. Curr Opin Chem Biol 9:674–679. doi:10.1016/j.cbpa.2005.10.005

Bosse D, Bart HJ (2005) Viscosity calculations on the basis of Eyring's absolute reaction rate theory and COSMOSPACE. Ind Eng Chem Res 44:8428–8435. doi:10.1021/ie048797g

Bryc W (2002) A uniform approximation to the right normal tail integral. Appl Math Comput 127:365–374. doi:10.1016/S0096-3003(01)00015-7

Chen X, Cao GX, Han AJ, Punyamurtula VK, Liu L, Culligan PJ, Kim T, Qiao Y (2008) Nanoscale fluid transport: size and rate effects. Nano Lett 8(9):2988–2992. doi:10.1021/nl802046b

David RL (2003–2004) CRC handbook of chemistry and physics, 84th edn. CRC Press, New York

Eyring H (1936) Viscosity, plasticity, and diffusion as examples of absolute reaction rates. J Chem Phys 4:283–291. doi:10.1063/1.1749836

Giovambattista N, Rossky PJ, Debenedetti PG (2009) Phase transitions induced by nanoconfinement in liquid water. Phys Rev Lett 102:050603. doi:10.1103/PhysRevLett.102.050603

Guo GJ, Zhang YG (2001) Equilibrium molecular dynamics calculation of the bulk viscosity of liquid water. Mol Phys 99(4):283–289. doi:10.1080/00268970010011762

Hallett J (1963) The temperature dependence of the viscosity of supercooled water. Proc Phys Soc 82:1046–1050. doi:10.1088/0370-1328/82/6/326

Han AJ, Lu WY, Punyamurtula VK, Chen X, Surani FB, Kim T, Qiao Y (2008) Effective viscosity of glycerin in a nanoporous silica gel. J Appl Phys 104:124908. doi:10.1063/1.3020535

Hanasaki I, Nakatani A (2006) Flow structure of water in carbon nanotubes: poiseuille type or plug-like? J Chem Phys 124(14):144708. doi:10.1063/1.2187971

Hans WH, William CS, Jed WP, Jeffry DM, Thomas JD, Greg LH, Teresa HG (2004) Development of an improved four-site water model for biomolecular simulations: TIP4P-EW. J Chem Phys 120(20):9665–9678. doi:10.1063/1.1683075

Henkelman G, Jónsson H (2000) A climbing image nudged elastic band method for finding saddle points and minimum energy paths. J Chem Phys 113:9978. doi:10.1063/1.1329672

Holt JK (2008) Methods for probing water at the nanoscale. Microfluid Nanofluid 5:425–442. doi:10.1007/s10404-008-0301-9

Holt JK, Park HG, Wang YM, Stadermann M, Artyukhin AB, Grigoropoulos CP, Noy A, Bakajin O (2006) Fast mass transport through sub-2-nanometer carbon nanotubes. Science 312:1034–1037. doi:10.1126/science.1126298

Horne RA, Courant RA, Johnson DS, Margosian FF (1965) The activation energy of viscous flow of pure water and sea water in the temperature region of maximum density. J Phys Chem 69(11):3988–3991. doi:10.1021/j100895a057

Hummer G, Rasaiah JC, Noworyta JP (2001) Water conduction through the hydrophobic channel of a carbon nanotube. Nature 414:188–190. doi:10.1038/35102535

Joseph S, Aluru NR (2008) Why are carbon nanotubes fast transporters of water? Nano Lett 8(2):452–458. doi:10.1021/nl072385q

Kalra A, Garde S, Hummer G (2003) Osmotic water transport through carbon nanotube membranes. Proc Natl Acad Sci 100(8):10175–10180. doi:10.1073/pnas.1633354100

Kauzmann W, Eyring H (1940) The viscous flow of large molecules. J Am Chem Soc 62(11):3113–3125. doi:10.1021/ja01868a059

Kincaid JF, Eyring H, Stearn AE (1941) The theory of absolute reaction rates and its application to viscosity and diffusion in the liquid state. Chem Rev 28(2):301–365. doi:10.1021/cr60090a005

Koga K, Gao GT, Tanaka H, Zeng XC (2001) Formation of ordered ice nanotubes inside carbon nanotubes. Nature 412:802–805. doi:10.1038/35090532

Lee MJ, Chiu JY, Hwang SM, Lin HM (1999) Viscosity calculations with the Eyring–Patel–Teja model for liquid mixtures. Ind Eng Chem Res 38(7):2867–2876. doi:10.1021/ie980751y

Lei QF, Hou YC, Lin RS (1997) Correlation of viscosities of pure liquids in a wide temperature range. Fluid Phase Equilibr 140:221–231. doi:10.1016/S0378-3812(97)00176-3

Li YX, Xu JL, Li DQ (2010) Molecular dynamics simulation of nanoscale liquid flows. Microfluid Nanofluid. doi:10.1007/s10404-010-0612-5

Liu YC, Wang Q, Wu T, Zhang L (2005) Fluid structure and transport properties of water inside carbon nanotubes. J Chem Phys 123:234701. doi:10.1063/1.2131070

Majumder M, Chopra N, Andrews R, Hinds BJ (2005) Enhanced flow in carbon nanotubes. Nature 438:44. doi:10.1038/438044a

Mallamace F, Branca C, Corsaro C, Leone N, Spooren J, Stanley HE, Chen SH (2010) Dynamical crossover and breakdown of the stokes-einstein relation in confined water and in methanol-diluted bulk water. J Phys Chem B 114:1870. doi:10.1021/jp910038j

Martí J (1999) Analysis of the hydrogen bonding and vibrational spectra of supercritical model water by molecular dynamics simulations. J Chem Phys 110(14):6876–6886. doi:10.1063/1.478593

Mashl RJ, Joseph S, Aluru NR, Jakobsson E (2003) Anomalously immobilized water: a new water phase induced by confinement in nanotubes. Nano Lett 3(5):589–592. doi:10.1021/nl0340226

Poling BE, Prausnitz JM, O'Connell JP (2001) The properties of gases and liquids. McGraw-Hill Companies, New York

Powell RE, Roseveare WE, Eyring H (1941) Diffusion, thermal conductivity, and viscous flow of liquids. Ind Eng Chem 33(4): 430–435. doi:10.1021/ie50376a003

Steve P (1995) Fast parallel algorithms for short-range molecular dynamics. J Comput Phys 117:1–19. doi:10.1006/jcph.1995.1039 (http://lammps.sandia.gov)

Sun YL, Sun MH, Cheng WD, Ma CX, Liu F (2007) The examination of water potentials by simulating viscosity. Comput Mater Sci 38:737–740. doi:10.1016/j.commatsci.2006.05.007

Thomas JA, McGaughey AJH (2008) Reassessing fast water transport through carbon nanotubes. Nano Lett 8(9):2788–2793. doi:10.1021/nl8013617

Tolman RC (1920) Statistical mechanics applied to chemical kinetics. J Am Chem Soc 42:2506

Velikov V, Borick S, Angell CA (2001) The glass transition of water based on hyperquenching experiments. Science 294:2335–2338. doi:10.1021/ja01457a008

Walter J, Moore JR, Eyring H (1938) Theory of the viscosity of unimolecular films. J Chem Phys 6:391–394. doi:10.1063/1.1750274

Walther JH, Jaffe R, Halicioglu T, Koumoutsakos P (2001) Carbon nanotubes in water: structural characteristics and energetics. J Phys Chem B 105:9980–9987. doi:10.1021/jp011344u

Wang HJ, Xi XK, Kleinhammes A, Wu Y (2008) Temperature-induced hydrophobic-hydrophilic transition observed by water adsorption. Science 322:80–83. doi:10.1126/science.1162412

Wonham J (1967) Effect of pressure on the viscosity of water. Nature 215:1053–1054. doi:10.1038/207620a0

Zhu FQ, Tajkhorshid E, Schulten K (2004) Collective diffusion model for water permeation through microscopic channels. Phys Rev Lett 93:224501. doi:10.1103/PhysRevLett.93.224501